^{187}Os–^{186}Os systematics of Os–Ir–Ru alloy grains from southwestern Oregon

R.J. Walker[a],*, A.D. Brandon[b], J.M. Bird[c], P.M. Piccoli[a], W.F. McDonough[a], R.D. Ash[a]

[a]Department of Geology, University of Maryland, College Park, MD 20742, USA
[b]NASA Johnson Space Center, Mail Code SR, Building 31, Room 114, Houston, TX 77058, USA
[c]4126 Snee Hall, Department of Earth and Atmospheric Sciences, Cornell University, Ithaca, NY 14853, USA

Abstract

More than 100 Os–Ir–Ru alloy grains from southwestern Oregon, presumably originating in the Mesozoic Josephine ophiolite, were examined for major and minor element compositions and ^{187}Os/^{188}Os isotopic compositions. Sixteen grains spanning the range of ^{187}Os/^{188}Os ratios present in the larger suite were analyzed for high-precision ^{186}Os/^{188}Os ratios. The ranges of major and minor element abundances of individual grains were, in general, similar to compositions previously reported for such grains worldwide. Within-suite compositional variations were quite large. Most grains were likely disaggregated from larger intergrown clusters, and were subdivided based on texture into matrix and lamellae. Composition variations within individual matrix grains were limited, whereas variations within individual lamellae grains were considerably larger.

The ^{187}Os/^{188}Os ratios of individual grains were isotopically homogeneous at the $\pm 0.1\%$ level of resolution. The ^{187}Os/^{188}Os ratios of the entire suite of grains ranged from 0.1173 to 0.1468. The average ratio for all grains combined was 0.1241, similar to the composition of three chromitites sampled from the Josephine Creek, and consistent with formation in the Mesozoic upper mantle. The average ^{186}Os/^{188}Os ratio of the subset of 16 grains was 0.119838. All grains but one had isotopic ratios within ± 20 ppm of that ratio.

Results indicate that ^{187}Os/^{188}Os variations on a scale of mm^3 may be quite large within the upper mantle, mimicking heterogeneities observed in both hand-and outcrop-scale samples of upper mantle materials. Highly depleted compositions relative to ambient upper mantle with chondritic ^{187}Os/^{188}Os require that some of the heterogeneities must be >1 Ga. The homogeneity of the ^{186}Os/^{188}Os ratios lend no support to the contention that isotopic heterogeneities within the upper mantle may explain coupled ^{186}Os–^{187}Os enrichments that have been observed in putative plume derived lavas.
© 2004 Elsevier B.V. All rights reserved.

Keywords: Os–Ir–Ru alloys; mantle; ^{186}Os/^{188}Os; ^{187}Os/^{188}Os

---

* Corresponding author. Tel.: +1 3014054089; fax: +1 3014053597.
E-mail address: rjwalker@geol.umd.edu (R.J. Walker).

1. Introduction

Osmium–iridium–ruthenium (Os–Ir–Ru) alloys are usually found in association with ultramafic rocks as either inclusions within minerals such as chromite (e.g. [1]), or as placers in streambeds draining terrains bearing ultramafic rocks [2,3]. The common occurrence of such alloys as placers is a result of the extreme resistance of the alloy grains to alteration and their very high densities (>20 g/cm^3).

The origin of Os–Ir–Ru alloy grains has been considered within two broad genetic frameworks: exogenous to the upper mantle and indigenous to the upper mantle. The possibility that at least some alloy grains form at very high temperatures has been interpreted as evidence for exogenous formation deep in the lower mantle or core [4]. Grains formed at such depths would somehow have to be transported to the upper mantle and ultimately exposed at the surface. As a consequence of their ultra-refractory nature and intergrown texture, this mode of origin was suggested for placer-derived Os–Ir–Ru grains found near Port Orford, in southwestern Oregon [4]. Two indigenous processes that have been proposed for the formation of alloy grains within the lithosphere are release and subsequent reduction of Os, Ir and Ru during alteration of sulfides, and direct precipitation in magma chambers [2,5–7]. For example, Brenker et al. [7] reported the occurrence of silicate and chromite inclusions within alloy grains collected largely from the same Port Orford placers examined by [4]. They concluded that the shapes and compositions of these inclusions are most consistent with magmatic formation of the alloy grains in the mantle wedge above a subduction zone.

The Os isotopic compositions of Os–Ir–Ru alloys (^{187}Re→^{187}Os, $t_{1/2}$=42 b.y.; ^{190}Pt→^{186}Os, $t_{1/2}$=430 b.y.) can provide diagnostic information about the origin of the alloys. The characteristic very low Re/Os and Pt/Os ratios of alloy grains mean that detectable ingrowth of radiogenic ^{187}Os and ^{186}Os ceased when the grains formed, so the Os isotopic composition of individual grains must reflect the long-term Re/Os and Pt/Os ratios of precursor materials. Indeed, analyses of Os–Ir–Ru alloys with different assumed formation ages have previously been used to characterize the Re–Os and Pt–Os isotopic evolution of the upper mantle [8–10].

For this study, a suite of Os–Ir–Ru grains collected from placer deposits near Port Orford are examined with respect to bulk composition, and ^{187}Os/^{188}Os and ^{186}Os/^{188}Os ratios. Care was taken to document chemical and isotopic heterogeneities within individual grains using both electron microprobe and laser ablation ICP-MS techniques. Our work was spurred by recent studies that reported coupled ^{186}Os–^{187}Os isotope systematics of alloy grains from southwestern Oregon and spatially associated northern California Os–Ir–Ru alloy occurrences [11–14]. These studies have reported supra-chondritic ^{186}Os/^{188}Os for most samples analyzed. The ^{187}Os–^{186}Os relations reported by these studies have been argued to be consistent with: (a) an outer core/lower mantle origin [11], (b) derivation from an "ancient" reservoir [12] or (c) derivation from upper mantle sources that are variably enriched in pyroxene [14]. In addition, Meibom et al. [13,14] cited the range in ^{187}Os/^{188}Os ratios of a suite of >700 alloy grains to conclude that the Os isotopic composition of the upper mantle is extremely heterogeneous on a small scale, consistent with previous isotopic heterogeneities observed via large-scale sampling of abyssal peridotites [15,16] and ophiolites [17–19].

Additional study of grains from southwestern Oregon is warranted because of their impact on the ongoing debate regarding interpretations of coupled ^{186}Os–^{187}Os trends in various volcanic suites, and with respect to the general evolution and distribution of Os isotopes in the upper mantle. Previous studies [10,20,21] concluded that coupled enrichments of ^{187}Os and ^{186}Os in Siberian and Hawaiian picrites and Gorgona Island komatiites most likely reflect the addition of outer core Os to the mantle sources of these rocks. Alternate interpretations for the coupled enrichments have also been tendered. For example, Ravizza et al. [22] argued that the coupled isotopic systematics observed in the Hawaiian picrites may result from contamination of upper mantle-or plume-derived materials with Pt-rich metalliferous sediments. Smith [23] concluded that the coupled trends observed for the Hawaiian picrites could reflect a derivation of some portion of the Os via partial melting of pyroxene-rich mantle rocks that are enriched in Pt. If sufficiently large, correlated enrichments of ^{186}Os and ^{187}Os can be proven to exist in the upper mantle, an interpretation of an upper mantle

origin for the Hawaiian, Siberian and Gorgona trends would likely be favored.

In order to further assess these models for ^{186}Os–^{187}Os variation for mantle materials and to address issues regarding data quality and reproducibility between labs, additional high precision Os isotope measurements on the same grains using two different mass spectrometers were made for this study. In addition, in situ ^{187}Os/^{188}Os ratio and corresponding compositional data were determined to examine variations within and among the grains as a means to evaluate petrogenetic models for the origins of the grains.

2. Samples

The collection of placer grains examined here is a subset of thousands of grains originally collected by Benjamin Silliman near Port Orford, Oregon that were
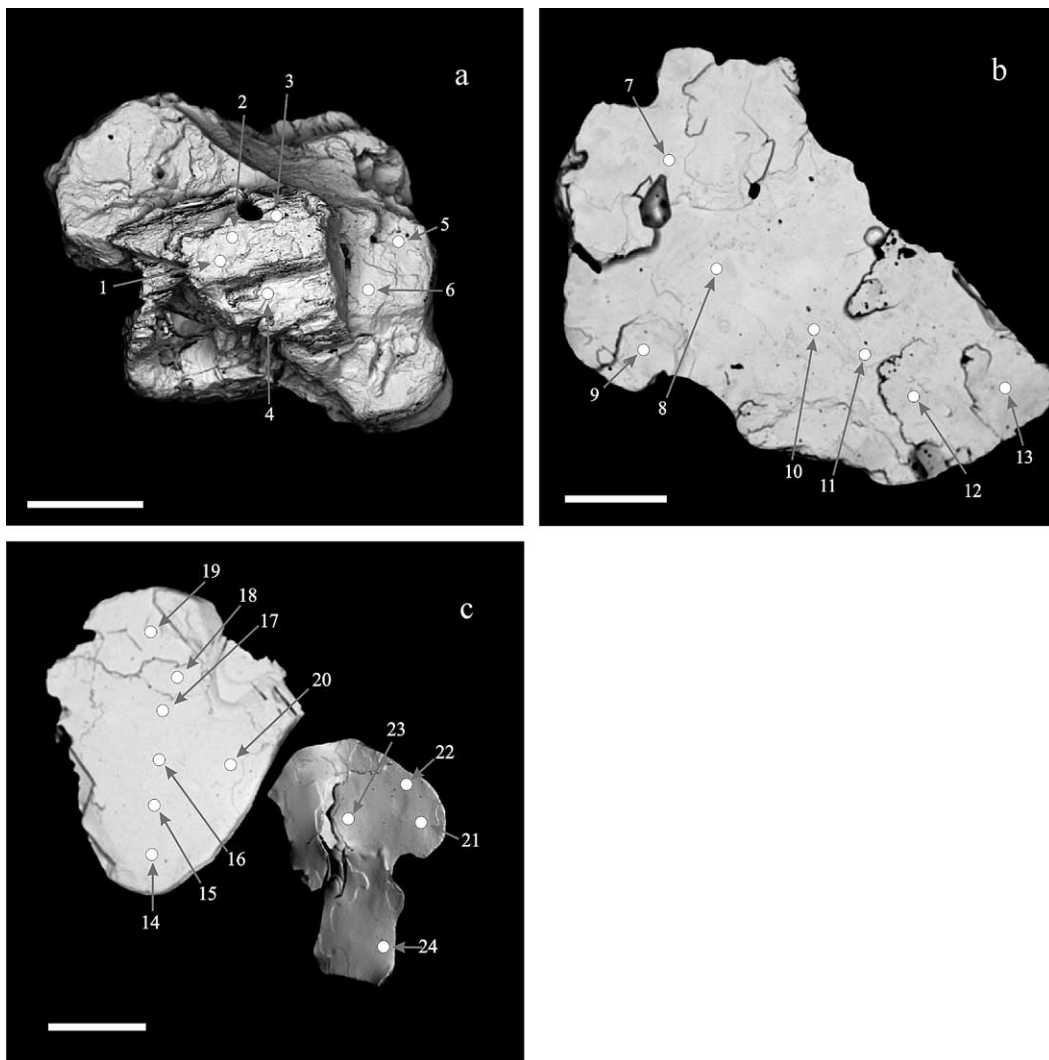

Fig. 1. Backscatter electron images (BSE) of CU 22-8 matrix grains analyzed as part of the 2002 analytical campaign. The bar in each image is 500 μm long. (a) Matrix grain M1. (b) Matrix grain M2. (c) Matrix grains M3 (left) and M4 (right). Numbered circles are locations of microprobe analysis.

added to the Yale Peabody Museum collection as sample number YPM MIN.1.182. In 1870, a subset of this sample was given to Cornell University. It was labeled "iridosmine, Port Orford, Oregon", and became sample CU 22-8 in the Cornell collection, the sample number cited here.

Additional grains of Os–Ir–Ru alloys were subsequently collected from placers in Josephine Creek, southwest Oregon in the 1970s [24], and were visually examined and found to be similar to CU 22-8. It is, therefore, likely that all of the grains examined here were derived from the ca. 162 Ma Josephine ophiolite that is drained by the Josephine Creek. Several alloy

grains from sample CU 22-8 have been previously analyzed for Os isotopes [11–14], and both [13,14] reported data for additional grains collected from the Josephine Creek location [24] and several other locales in northern California and southwestern Oregon. Field relations among the locales where grains have been sampled were most recently reviewed in [13,14].

All of the grains examined here were single, subhedral to euhedral crystals or platy fragments. All were less than 1–2 mm in largest dimension (Figs. 1 and 2) and all were likely derived from intergrown alloy clusters [4]. One such cluster was analyzed here for Os isotopes. Previous studies (e.g. [11]) have
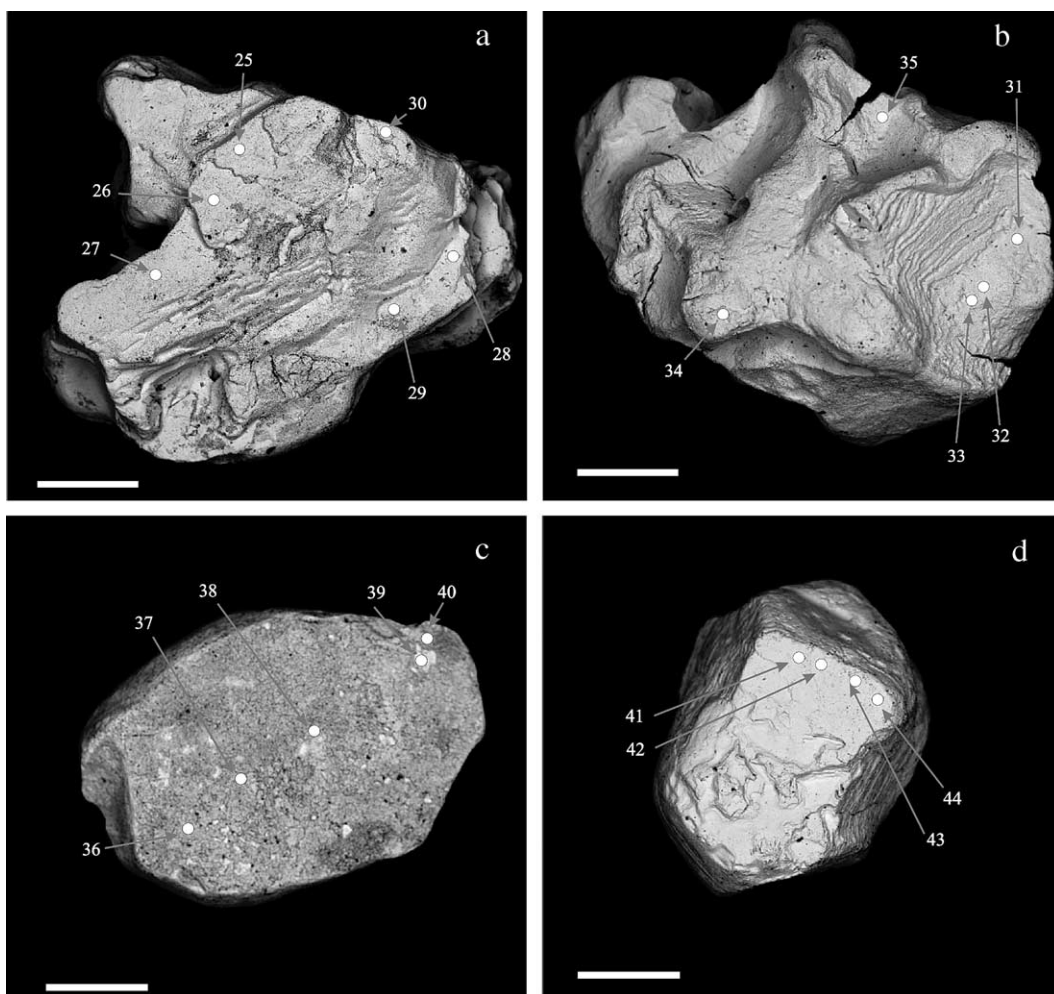

Fig. 2. Backscatter electron images (BSE) of CU 22-8 lamellae analyzed as part of the 2002 analytical campaign. The bar in the image is 500 μm long. (a) Lamellae grain L1. (b) Lamellae grain L2. (c) Lamellae grain L3. (d) Lamellae grain L4. Numbered circles are locations of microprobe analysis.

subdivided grains presumably disaggregated from clusters into textural groups of "matrix" and "lamellae"; all grains examined here are defined based on texture as portions of either lamellae or matrix.

Three water rounded chromitite pebbles (JOS1, JOS2 and JOS3) were collected from the streambed of the Josephine Creek. Like the alloy grains, these rocks were undoubtedly derived from the ultramafic terrains that are drained by this creek.

3. Analytical techniques

Os–Ir–Ru alloy grains from the Cornell CU 22-8 collection were analyzed during the course of two campaigns conducted in 2002 and 2003. Major and minor element concentrations of all grains were determined using a JEOL 8900 Electron Probe Microanalyzer at the University of Maryland (Table 1). For a subset of 16 grains, multiple spots were analyzed in order to assess within-grain chemical homogeneity (Table 2; Figs. 1 and 2). Unpolished matrix and lamellae grains were mounted on carbon tape (a requirement due to the subsequent dissolution required for some specimens), and analyzed using standard wavelength dispersive spectroscopy (WDS) techniques for Fe, Ru, Rh, Pd, W, Re, Os, Ir, Pt and, for some grains, Ni. Pure element standards were used, with the exception of Os where an OsIr alloy (63.2% Os:26.8% Ir) was used in order to avoid interfaces in pure Os metal, and due to the absence of a large, pore-free pure Os standard.

The large number of closely spaced x-ray lines for many of these elements led to a protocol where qualitative WDS scans were performed on several randomly chosen grains, in addition to standards, in order to identify peak and background positions where minimal overlap would obtain. In an attempt to evaluate possible errant concentrations, standards were subsequently analyzed as unknowns to ensure peak and background positions were correct. Where necessary, WDS of pure metal standards were analyzed in order to determine appropriate overlap corrections. The following X-ray lines were used: K_α (Fe, Ni), L_α (Ru, Rh, W, Re, Os, Ir and Pt) and L_β (Pd). Operating conditions were as follows: accelerating voltage of 25 keV, sample current of 50 nA, 1 μm beam diameter, count times ranging between 10 and

Table 1

Major and minor element chemistry of matrix and lamellae grains as determined by electron probe microanalysis (concentrations in wt.%)

Analysis set 1

	M1	M2	M3	M4	L1	L2	L3	L4
Pt	2.07	0.99	2.34	1.47	0.66	6.47	1.70	0.13
W	b.d.	b.d.	b.d.	b.d.	0.08	b.d.	0.41	b.d.
Rh	0.62	0.42	0.67	0.49	0.44	0.42	0.33	0.14
Os	44.01	54.82	42.62	41.49	40.89	31.46	39.99	66.94
Re	b.d.	b.d.	b.d.	b.d.	b.d.	b.d.	b.d.	b.d.
Ru	13.40	6.15	14.10	13.17	14.15	1.23	11.27	2.58
Ir	37.08	36.39	36.68	31.29	37.83	60.90	33.83	27.97
Ni	n.a.	n.a.	n.a.	n.a.	n.a.	n.a.	n.a.	n.a.
Fe	0.12	0.24	0.26	0.28	2.55	0.39	5.04	0.66
Pd	0.13	0.08	0.02	0.06	0.04	0.07	2.84	0.95
Total	97.44	99.09	96.71	88.27	96.65	100.93	95.41	99.39

Analysis set 2

	M5	M6	M7	M8	L5	L6	L7	L8
Pt	2.23	0.32	3.19	3.62	1.96	b.d.	b.d.	b.d.
W	b.d.	b.d.	b.d.	b.d.	b.d.	b.d.	0.55	0.33
Rh	0.49	0.54	0.78	0.48	0.52	0.18	0.36	0.26
Os	44.36	53.71	37.26	43.26	72.60	52.33	44.51	33.08
Re	b.d.	b.d.	b.d.	b.d.	b.d.	b.d.	b.d.	b.d.
Ru	13.62	6.82	16.16	14.66	5.67	5.83	10.28	8.39
Ir	33.37	36.50	36.50	34.35	15.37	34.20	33.50	45.36
Ni	0.04	0.02	b.d.	b.d.	b.d.	0.03	b.d.	0.02
Fe	0.44	0.26	0.22	0.05	0.18	0.90	3.67	7.19
Pd	0.20	0.06	0.01	0.01	0.18	0.34	0.64	0.64
Total	94.74	98.23	94.14	96.47	96.50	93.80	93.51	95.27

Columns titled M1–M4 and L1–L4 correspond to average compositions of matrix and lamellae grains shown in Figs. 1a–c and 2a–d, respectively.

Abrreviations are as follows: n.a.—not analyzed, b.d.—below detection. Detection limits based on counting statistics only are as follows (2σ, in ppm): Pt (1800), W (270), Rh (140), Os (1550), Re (600), Ru (150), Ir (1800), Pd (180) and Ni (200).

30 s (on peak), and 2–10 analyses per grain (depending on size and topography). X-ray intensities were corrected using the CIT-ZAF algorithm.

The grains were subsequently analyzed for $^{187}Os/^{188}Os$ ratio via in situ measurements using a laser ablation system coupled to a *Nu Plasma* multicollector inductively-coupled plasma-mass spectrometer (MC-ICP-MS). Spot analyses were conducted for some of the same locations in the grains analyzed by electron microprobe. Particular emphasis was placed on the isotopic analysis of spots that displayed significant within-grain compositional heterogeneity. The MC-ICP-MS was teamed with a

Table 2
Representative variation in select host and lamellae grains (concentrations in wt.%)

Matrix grain M1

Spot no.	1	2	3	4	5	6
Pt	2.39	2.20	2.06	1.79	1.78	2.20
W	b.d.	b.d.	b.d.	b.d.	b.d.	b.d.
Rh	0.54	0.55	0.62	0.59	0.73	0.70
Os	47.21	47.27	43.10	42.91	41.77	41.82
Re	b.d.	b.d.	b.d.	b.d.	b.d.	b.d.
Ru	11.40	11.35	13.42	13.41	15.37	15.43
Ir	36.71	36.39	38.27	37.80	36.84	36.47
Fe	0.10	0.10	0.18	0.18	0.09	0.09
Pd	0.08	0.08	0.26	0.22	0.08	0.09
Total	98.42	97.94	97.92	96.90	96.65	96.80

Lamellae grain L3

Spot no.	36	37	38	39	40
Pt	7.54	b.d.	b.d.	0.58	0.36
W	b.d.	0.41	0.48	0.59	0.57
Rh	0.46	0.27	0.20	0.36	0.37
Os	29.40	38.76	44.57	43.66	43.57
Re	b.d.	b.d.	b.d.	b.d.	b.d.
Ru	0.91	12.57	11.61	15.67	15.58
Ir	62.36	28.80	29.91	23.84	24.26
Fe	0.25	4.96	4.49	7.73	7.756
Pd	0.02	12.29	1.43	0.22	0.23
Total	100.94	98.06	92.70	92.65	92.70

laser ablation system consisting of a *New Wave Research* UP 213 laser, which uses a Q-switched, Nd:YAG crystal and a set of harmonic optics to achieve a monochromatic beam of 213 nm light. The specific settings for the instruments used in this experiment are listed in Table 3. Ion beam currents were collected in a single, static mode, acquisition cycle using multiple Faraday buckets. Following a peak centering routine, background measurements were taken at the high and low half mass positions, with off-peak positioning achieved by 10 V deflections applied to the electrostatic analyzer. Background spectra were accumulated for 5 s at each position prior to each data sequence; an average of these two spectra was used as the background for peak processing. On-peak backgrounds were monitored between analyses and were always equivalent to the half mass values. Potential isobaric interferences (i.e., ^{186}W, ^{187}Re and $^{190,192}Pt$) were monitored throughout each analysis by collecting data at mass 182, 185 and 194. Measured ion currents at masses

182 and 185 were always equivalent to the background values. Measured ion currents at mass 194, which are assumed to be ^{194}Pt (32.93%) contributions, were used to subtract the minor contributions of ^{192}Pt (0.80%) and ^{190}Pt (0.014%) from the Os spectrum. The minor to negligible Pt contributions to the Os spectrum had little to no effect on the final $^{187}Os/^{188}Os$ values. In all cases, 2σ in-run statistics were $\leq\pm0.1\%$. Also in all cases, $^{187}Os/^{188}Os$ measured by laser ablation matched the ratio measured by acid digestion and negative thermal ionization mass spectrometry (NTIMS) analysis within $\pm0.2\%$.

As a final step, the 16 grains chosen for ^{186}Os analysis (8 for the first campaign and 8 for the second) were dissolved in acid inside sealed Carius tubes, and Os was purified via solvent extraction and microdistillation for NTIMS. Purified Os was analyzed for

Table 3
Operating conditions for laser ablation analysis of Os using *Nu Plasma* ICP-MS

RF forward (27.12 MHz)	1350 W
Cool gas flow	14 l/min Ar
Auxillary gas flow	0.9 l/min Ar
Ablation cell gas flow	0.6 l/min He
Supplemental ablation gas flow	0.7 l/min Ar
Sample cone (Ni) orifice	1.1 mm
Skimmer cone (Ni) orifice	0.7 mm
$m/\Delta m$	300
Extraction potential	4012 V
Analysis acquisition mode	static
Ion detection mode	Faraday cups
Configuration of Faraday cups:	^{194}Pt (H6)
^{192}Os (H5)　　　^{190}Os (H4)	^{189}Os (H3)
^{188}Os (H2)　　　$^{187}Os+^{187}Re$ (H1)	^{186}Os (Ax)
^{185}Re (L1)　　　^{184}Os (L2)	^{182}W (L3)
Integration time	2 s
Magnet settling time	2 s
Number of ratios per run	20
Ion beam current for ^{192}Os	1–9 EA
Normalization value $^{189}Os/^{188}Os$	3.08271
Mass fractionation law	exponential
UP213 (laser ablation system)	
Fundamental light (Nd:YAG)	λ=1064 nm
5th harmonic	λ=213 nm
Pulse duration	5 ns
Output power on sample	1–1.5 J/cm^2
Spot size (diameter)	30–60 μm
Pulse repartition rate[a]	5, 6 and 8 Hz

[a] Pulse frequency optimized for maximum signal intensity on ^{192}Os.

high precision $^{187}Os/^{188}Os$ and $^{186}Os/^{188}Os$ ratios at both the University of Maryland (UMd) and Johnson Space Center (JSC), Houston. Details of analytical techniques used are as follows.

The chemical separation and NTIMS techniques used at the UMd have been previously detailed [20]. In brief, grains were sealed in Pyrex Carius tubes with approximately 4 g concentrated HNO_3 and 2 g concentrated HCl, then heated at 240 °C for >24 h. This technique resulted in partial or complete digestion of the grains. $^{187}Os/^{188}Os$ and $^{186}Os/^{188}Os$ ratios were measured with a three-stage peak hopping routine. Baselines were measured at half-mass positions. The intensity of the ^{186}Os beam, measured as $^{-186}Os^{16}O_3$ at mass 234, was maintained at a constant 150 mV. Possible W interferences were monitored during each run using an electron multiplier at mass 231 ($^{-183}W^{16}O_2$) and by monitoring $^{184}Os/^{188}Os$. No W corrections were necessary, as is consistent with the very different ionization characteristics of negatively charged molecular species of W and Os. The averages

for the Johnson-Matthey Os standard were 0.1198520 ± 22 and 0.1198485 ± 15 (2σ SDM) for $^{186}Os/^{188}Os$ for the two campaigns, respectively.

At the Johnson Space Center, the high-precision measurements of the $^{186}Os/^{188}Os$–$^{187}Os/^{188}Os$ isotopic compositions were performed by N-TIMS in static mode on an eight-Faraday collector *Thermo-Finnigan Triton*® mass spectrometer. Signals of 150–250 mV on mass 234 ($^{186}Os^{16}O_3$) and 235 ($^{187}Os^{161}O_3$) were generated for 180 or greater ratios to reach the desired within run precision of ±0.0000015 or better for the $^{186}Os/^{188}Os$ ratio. Each cycle had an integration time of 17 s followed by a 4-s settling time. The possible isobaric interference of $^{186}W^{16}O_3$ on $^{186}Os^{16}O_3$ was monitored by measuring $^{184}Os^{16}O_3$ ($^{184}W^{16}O_3$) and was never observed. Oxygen corrections were made using the oxygen isotopic composition measured on 2-ng loads of ReO_4 on the faraday cups. Only one bottle of oxygen has been used to bleed O_2 into the Triton source from 2002 to 2004, and the oxygen isotopic composition during the

Table 4
Osmium isotopic data for Os–Ir–Ru alloys collected from near Port Orford, Oregon, and chromitite JOS-3, collected from Josephine Creek

Sample	$^{186}Os/^{188}Os_{(UMd)}$	2σ	$^{186}Os/^{188}Os_{(JSC)}$	2σ	Δ (ppm)	$^{186}Os/^{188}Os_{(Average)}$	$^{187}Os/^{188}Os_{(UMd)}$	2σ	$\gamma_{Os(162)}$
Analysis set 1									
M1	0.1198374	±53	0.1198403	±2	−29	0.1198389	0.1242810	±31	−1.3
M2	0.1198399	±20	0.1198390	±9	9	0.1198394	0.1244866	±40	−1.1
M3	0.1198370	±25	0.1198352	±25	18	0.1198361	0.1228417	±52	−2.4
M4	0.1198396	±21	0.1198390	±66	6	0.1198393	0.1261370	±40	0.2
L1	0.1198434	±26	0.1198363	±12	71	0.1198399	0.1227223	±47	−2.5
L2	0.1198402	±27	0.1198382	±7	20	0.1198392	0.1222315	±46	−2.9
L3	0.1198375	±34	0.1198408	±10	−33	0.1198392	0.1468146	±40	16.6
L4	0.1198389	±21	0.1198388	±17	1	0.1198388	0.1314007	±20	4.4
JOS3	0.1198381	±23					0.1259480	±160	
Analysis set 2									
L5	0.1198348	±47	0.1198394	±7	−46	0.1198371	0.1411853	±30	12.2
L6	0.1198351	±33	0.1198374	±8	−23	0.1198362	0.1294997	±54	2.9
L7	0.1198386	±7	0.1198370	±5	16	0.1198378	0.1207548	±44	−4.1
L8	0.1198385	±50	0.1198393	±9	−8	0.1198389	0.1208927	±42	−4.0
M5	0.1198363	±11	0.1198374	±9	−11	0.1198369	0.1273749	±23	1.2
M6	0.1198344	±38	0.1198396	±8	−52	0.1198370	0.1228463	±23	−2.4
M7	0.1198299	±31					0.1174193	±116	−6.7
M8	0.1198395	±23	0.1198378	±3	17	0.1198387	0.1260988	±55	0.2

All data were determined by NTIMS on bulk samples. M—matrix, L—lamellae. Each datum represents an average of two to six separate analyses of each sample and the 2σ value is the standard deviation of the population.
All analyses are corrected to a value of $^{186}Os/^{188}Os=0.1198476$ for the UMd standard. Δ is the difference in ppm between UMd-JSC measurements. $\gamma_{Os(162)}$ is the % deviation in $^{187}Os/^{188}Os$ from the chondritic reference at 162 Ma.

test runs throughout this period using ReO_4 has been constant. The O_2 pressures in the source were maintained in the range of $2-3 \times 10^{-7}$ mbar for all runs. After oxygen corrections were performed on the raw data, instrumental mass fractionation was corrected using $^{192}Os/^{188}Os = 3.083$ and the exponential law. Statistics were then applied to eliminate data beyond $\pm 2\sigma$ for each run. For all of the data reported in Table 4, two to six replicate runs of each sample were made and the average for each sample is reported with $\pm 2\sigma/n^{1/2}$ uncertainty. The data were obtained during two analytical campaigns—November 2002 and December 2003. The averages for the Johnson-Matthey Os standard was 0.0013096 ± 54
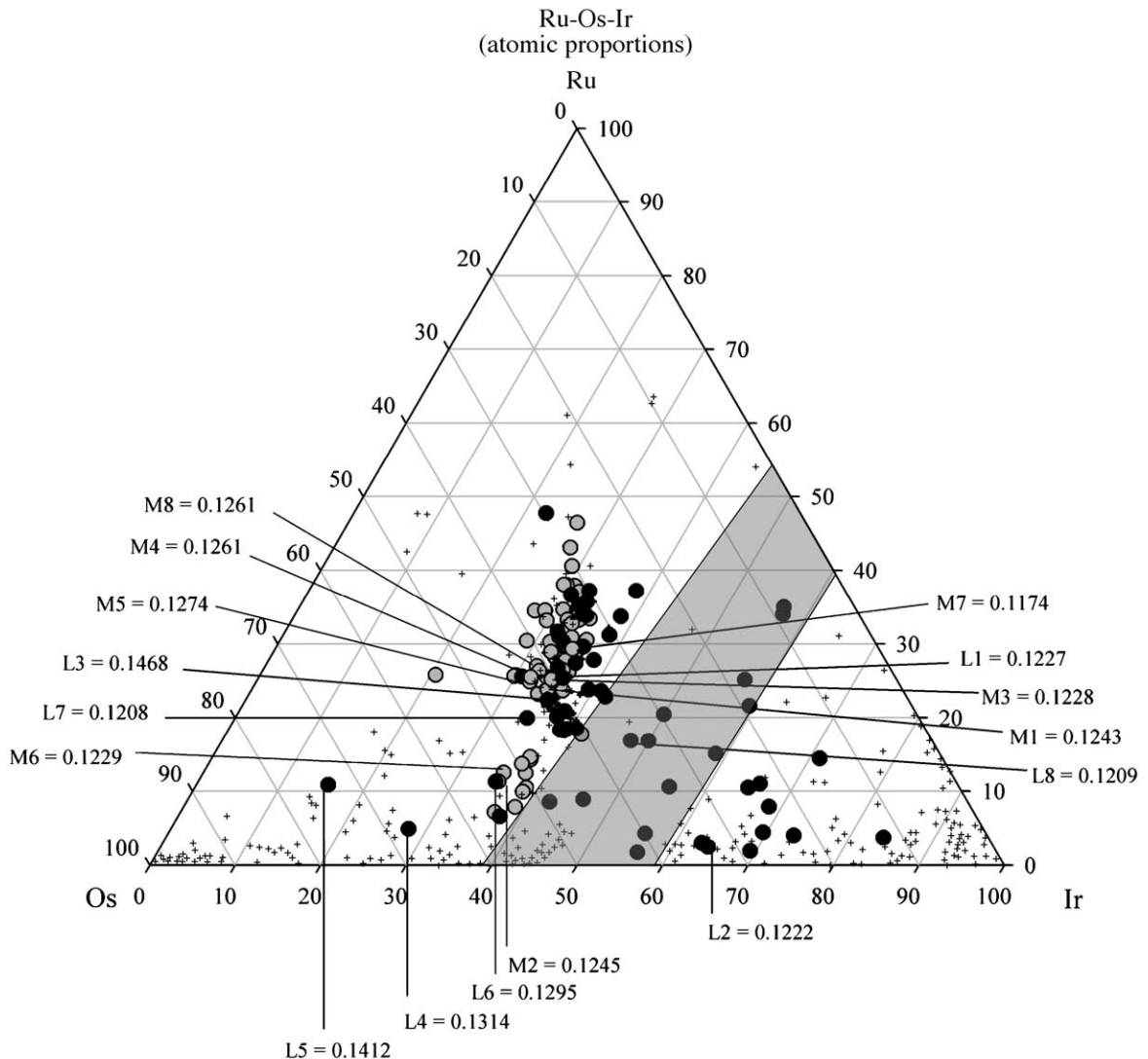
Fig. 3. Plot of the composition of lamellae (black circles) and matrix (gray circles) grains in Ru–Os–Ir space (atomic). Also plotted for comparison are select published analyses of alloy grains from worldwide locations (plus signs) from Harris and Cabri [27] and Feather [25]. The gray field is the estimated ternary miscibility gap based on the binary systems Ru–Os and Ru–Ir of Massalski [43]. The $^{187}Os/^{188}Os$ ratios for samples analyzed for both $^{186}Os/^{188}Os$ and $^{187}Os/^{188}Os$ are shown. There is no observable correlation between elemental composition and isotopic composition. It should be noted that although attempts were made to analyze matrix or lamellae exclusively, in some instances analyses may represent a mixture of both. All microprobe data can be accessed as a supplemental electronic file at doi:10.1016/j.epsl.2004.11.009.

(2σ) and 0.0013083±56 for [184]Os/[188]Os, 0.1198462±21 and 0.1198475±18 for [186]Os/[188]Os, and 0.1137891±44 and 0.1137920±24 for [187]Os/[188]Os, for 10//02–1/03 (*n*=23), and 8/03–12/03 (*n*=22), respectively. Data for samples from each analytical campaign (at both UMd and JSC) were corrected to a common [186]Os/[188]Os ratio of 0.1198476 for the UMd J-M standard.

Analyses of bulk chromitite samples for Re–Os systematics were done as per the methods of [19] at the UMd. One 2-g unspiked aliquant of chromitite was separately digested and analyzed repeatedly for high-precision [186]Os/[188]Os. Chemical and mass spectrometric techniques were the same as for the alloys.

4. Results

The range of bulk compositions defined by 118 grains is generally similar to that reported previously for worldwide occurrences of Os–Ir–Ru alloys, but are biased toward higher Ru content than most (e.g. [3,25,26]) (Tables 1 and 2; Fig. 3). Most grains examined are *ruthenirodosmines*, following the nomenclature proposed by [27], although there are also some grains of *iridosmine*, *ruthenosmiridium* and *osmiridium* within the suite. Overall, the major and minor element compositions of the matrix grains are much more restricted than those of the lamellae. For example, the Ir content of matrix grains generally
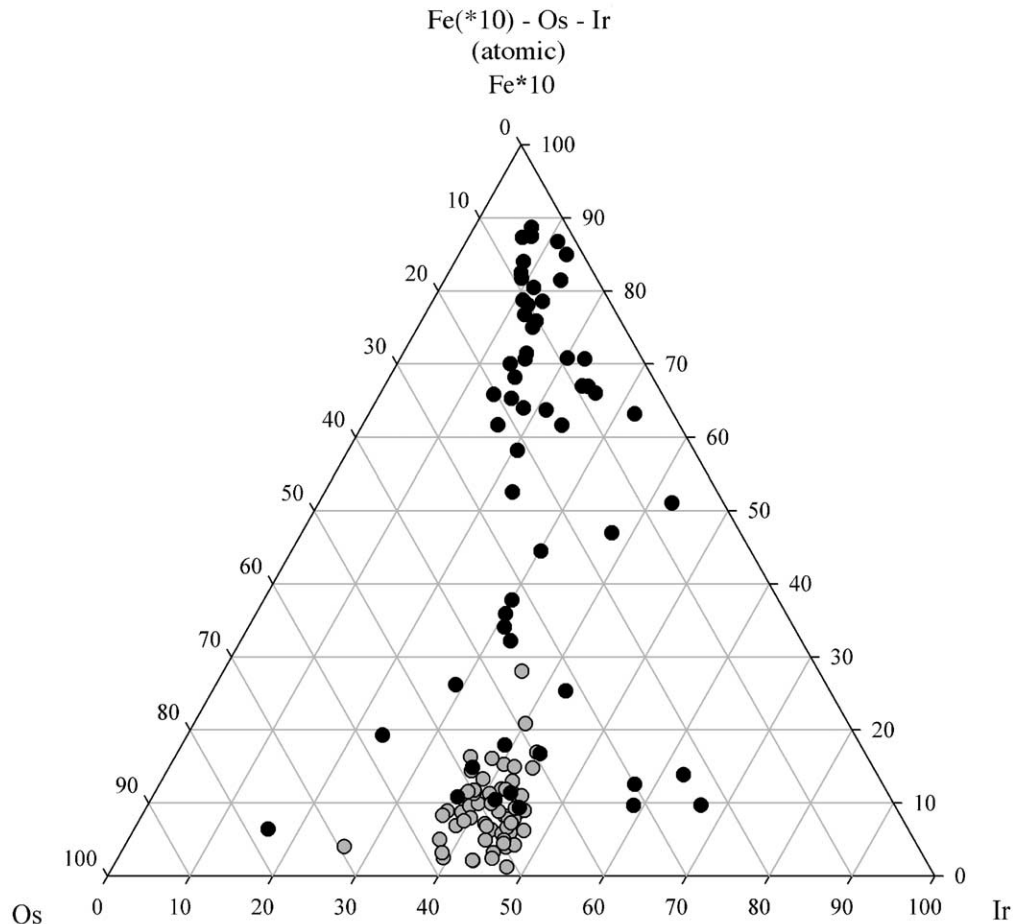

Fig. 4. Plot of the composition of grains in Fe(×10)–Os–Ir space (atomic). Symbols are as follows: lamellae (black circles), matrix (gray circles). Notice that the lamellae are generally more enriched in Fe compared with the matrix.
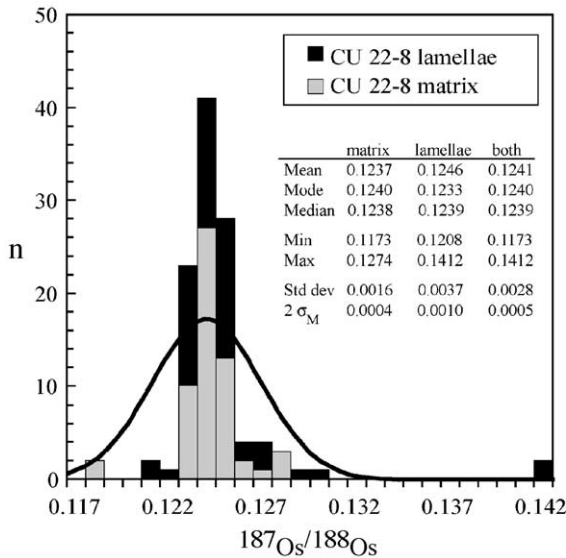
Fig. 5. Histogram of laser ablation ICP-MS $^{187}Os/^{188}Os$ ratio data for all Os–Ir–Ru grains examined by this study. All of these data can be accessed as a supplemental electronic file at doi:10.1016/j.epsl.2004.11.009.

ranges from 25% to 40% (atomic), but in lamellae, values cluster around the same locus, but extend continuously to values over 70%. The Ru/Os ratios of both matrix and lamellae are rather variable with values ranging from 1.5 to 0.

Grains optically identified as matrix tend to have lower Fe than grains optically identified as lamellae, with matrix grains having restricted Fe (≤0.02%), and generally subequal amounts of Os and Ir (Fig. 4). Lamellae contain up to an order of magnitude more Fe, and unlike the matrix grains, a significant number have Ir>Os (up to Ir/Os~9 at high Fe concentrations). Overlap between the composition fields of matrix and lamellae may reflect the presence of minor lamellae in matrix grains and vise-versa.

Individual grains are generally homogeneous with respect to major elements, although some portions of some grains show large variations in, for example, Os/Ir or Os/Ru. These ratios vary by as much as a factor of 12 in some samples (Table 2). The large differences in composition within individual grains again likely reflect the presence of both matrix and lamellae. Heterogeneities with respect to Os, Ir and Ru normally correlate with major changes in Fe content, consistent with this interpretation (e.g. grain L3, Table 2).

Rhenium was below the detection limit (<0.06 wt.% 2σ) for all analyses of all grains. Consequently, the effects of ingrowth of ^{187}Os with time are minute. The concentrations of minor platinum-group element constituents, Pt, Rh and Pd, vary by as much as a factor of 3 within individual grains. Platinum concentrations were sufficiently low that there has been no measurable ingrowth of ^{186}Os resulting from ^{190}Pt decay, regardless of the age of the grains.

The $^{187}Os/^{188}Os$ ratios of the entire suite of grains range from 0.1174 to 0.1468 (Fig. 5). For individual grains analyzed in multiple locations by LA-ICP-MS, there were no resolvable (>0.1%) variations in $^{187}Os/^{188}Os$ ratios. Hence, despite variations in major and minor element concentrations, the $^{187}Os/^{188}Os$ ratios of individual grains are uniform. A "cluster" containing both lamellae and matrix, previously discussed by [4], was also analyzed via LA-ICP-MS. This is the only sample where analysis of demonstrably coexisting lamellae and matrix was clearly resolved. All lamellae and matrix points analyzed for this sample had a uniform $^{187}Os/^{188}Os$ of 0.1243 ± 1. Because it is a rare cluster, it was not dissolved and analyzed at a higher precision by NTIMS.

The total range in $^{187}Os/^{188}Os$ ratios is similar to the range reported by [14], although that study

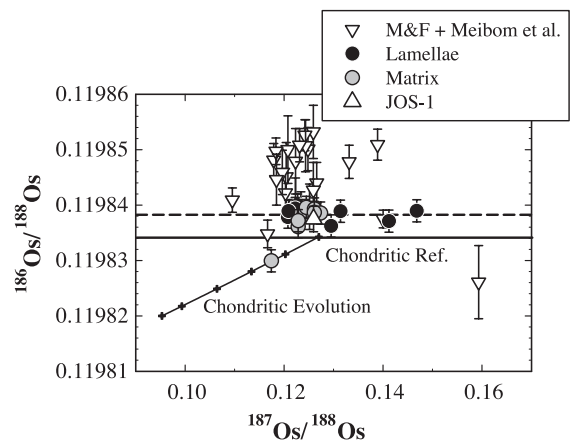Fig. 6. $^{186}Os/^{188}Os$ versus $^{187}Os/^{188}Os$ for Os–Ir–Ru grains. $^{186}Os/^{188}Os$ ratios plotted are the UMd-JSC averages (Table 4). The average $^{186}Os/^{188}Os$ ratio for 15 of 16 grains measured is shown as a dashed line. The chondritic average of Walker et al. [10] is shown as a solid line. The data of Meibom and Frei [12] and Meibom et al. [14] are shown for comparison. Chondritic evolution of ^{186}Os–^{187}Os is shown for comparison with crosses at 4.55, 4.0, 3.0, 2.0, 1.0 and 0 Ga.

reported several grains with higher and lower ratios than measured here. The average $^{187}Os/^{188}Os$ ratio of our matrix grains (n=57) is 0.1237±16 (1σ S.D.). The average $^{187}Os/^{188}Os$ ratio of lamellae grains (n=53) is 0.1246±37 (1σ S.D.). The average for all grains combined is 0.12413. This ratio is very similar to the average of 0.1245 reported for >700 grains analyzed by [13]. The combined population of lamellae and matrix grains show a gaussian distribution, with coincidence of median, mean and mode values (Fig. 5), and no distinguishing aspects to either population of grains. The similarity in distributions between the grains studied here and the grains examined by [13,14] is consistent with very similar sample populations.

Agreement between UMd and JSC $^{186}Os/^{188}Os$ measurements was quite good. The largest deviation was 71 ppm, with most deviations <30 ppm (Table 4). The isotopic variability in $^{186}Os/^{188}Os$ among the 16 grains analyzed by NTIMS was minimal (Table 4, Fig. 6). Combined UMd and JSC data, excluding sample M7, yield an average $^{186}Os/^{188}Os$ of 0.1198382±6 (2σ SDM). Sample 4–4 #7 has distinctly subchondritic $^{186}Os/^{188}Os$ and $^{187}Os/^{188}Os$ ratios. It plots on the chondritic evolution trajectory for $^{186}Os–^{187}Os$. All $^{186}Os/^{188}Os$ ratios (except sample M7) are within ±20 ppm of the mean ratio. The $^{186}Os/^{188}Os$ ratio results for the present study are in contrast to the much greater range of $^{186}Os/^{188}Os$ ratios previously reported for similar grains [12,14]. The average for the combined data of those two studies is 0.1198449±26 (2σ SDM, n=24). This ratio was obtained via normalization of the published data to higher $^{186}Os/^{188}Os$ by 22 ppm to account for the lower ratio measured by these workers (0.119845) for the same standard used for our new measurements.

The three chromitites from the Josephine Creek have initial $^{187}Os/^{188}Os$ ratios that range only from 0.1247 to 0.1252, assuming formation at 162 Ma [28] (Table 5). These ratios are within 1% of the average

ratio for all of the grains. Corresponding $\gamma_{Os(162)}$ values range from −0.99 to −0.55 (where $\gamma_{Os(162)}$ is the % deviation from chondritic average at 162 Ma [29]). The one chromitite processed for high precision isotope ratio measurement has $^{186}Os/^{188}Os$ and $^{187}Os/^{188}Os$ ratios of 0.1198381±23 and 0.1250963±90, respectively (Table 4). Both ratios are generally similar to the average values for the alloy grain suite.

5. Discussion

5.1. Major element compositions

Based on experimental studies [26] and studies of natural Os–Ir–Ru alloys [3,4], it has been proposed that a miscibility gap exists for the Os–Ir–Ru system between ~45% and 58% Os. All of the matrix grains collected as part of this study plot on the Os-rich side of the proposed miscibility gap. Lamellae compositions, however, range nearly continuously from ~30% to 70% Os, crossing the proposed gap. There is a paucity of grains with compositions between 50% and 58% Os, so it is unclear if the composition range can be continuous across the gap, or if a small gap exists. Possible reasons for a reduced volume of the miscibility gap include different P, T, fS_2 and fO_2, and substitution of weight percent quantities of Rh and Pt into the alloys. It is also possible that some analyses of lamellae reside in the miscibility gap because of beam overlap with included matrix that could bias an analysis towards higher Os+Ru.

5.2. $^{187}Os/^{188}Os$ ratios

The average $^{187}Os/^{188}Os$ ratio of 0.1241 obtained for the entire suite of Os–Ir–Ru alloy grains is only 0.7% lower than the average initial ratio for the three chromitites examined. Therefore, it is likely the chromitites have incorporated Os from a very similar provenance as the alloy grains.

It is now important to consider the age of the Josephine ophiolite with respect to Os isotope systematics. An age of 162±2 Ma for the Josephine ophiolite has been established via $^{40}Ar–^{39}Ar$ and U–Pb geochronology of mafic portions of the ophiolite [28]. Harper et al. [28] concluded that this age is the

Table 5
Rhenium–Os isotopic data for Josephine Creek chromitites

Sample	Re (ppb)	Os (ppb)	$^{187}Os/$ ^{188}Os	$^{187}Re/$ ^{188}Os	$^{187}Os/$ $^{188}Os_{(162)}$	$\gamma_{Os(162)}$
JOS1	0.350	67.61	0.12503	0.0249	0.12496	−0.77
JOS2	0.667	126.5	0.12475	0.0254	0.12469	−0.99
JOS3	0.167	75.33	0.12526	0.0107	0.12523	−0.55

magmatic crystallization age of mafic portions of the ophiolite, and therefore presumably the time of construction of this portion of the putative oceanic lithosphere that it samples. Emplacement of the ophiolite likely happened about 10 m.y. later, based on the ages of cross-cutting calc-alkaline dikes and plutons [28].

If the 162 Ma age also reflects the time of melt depletion of the ultramafic portion of the Josephine ophiolite, then the three chromitites and the average of the alloy grains have $^{187}Os/^{188}Os$ ratios that are about 3% below the Os isotope evolution trajectory defined by chromitites derived from other Phanerozoic ophiolites [19]. It is also possible the formation age of the ultramafic portions of the ophiolite, from which the chromitites and presumably the grains were derived, is greater than the age of the mafic portions of the ophiolite. It is normally difficult to test this age relation in any ophiolite because of the limited means for precisely determining the ages of peridotites. Osmium isotopes are often used for this task in constraining melt depletion ages for Proterozoic and Archean peridotites (e.g. [30,31]). The average Os model age for the grains and chromitites, calculated based on an assumption of derivation from a mantle reservoir evolving like the chondritic average [29] is ~300 Ma.

The $^{187}Os/^{188}Os$ ratios for the alloy grains examined extend from 0.1174 to 0.1468, a range of ~23% (γ_{Os}: −7.6 to +15.6). If the alloy grains formed in the upper mantle, this range suggests that with respect to $^{187}Os/^{188}Os$, the upper mantle is quite heterogeneous on a micro-scale, as previously noted for Os–Ir–Ru alloy grains [13,14,32], and chromite grains from abyssal peridotites [33]. Large Os isotopic heterogeneities have also been previously recognized for upper mantle-derived materials on scales ranging from hand-sample to outcrop, as observed in abyssal peridotites [15,16,33,34] and in peridotitic portions of individual ophiolites [18,35,36].

There are numerous probable causes of $^{187}Os/^{188}Os$ heterogeneities within the upper mantle. On a global scale, much of the Os isotopic heterogeneity within the upper mantle was likely caused by the same processes that have generated Pb, Nd, Hf and Sr isotopic heterogeneities. Processes such as melt removal, subduction-related crustal recycling, and metasomatism have led to changes in the Re/Os ratios

of domains within the upper mantle, and over time resulted in isotopic variations [29,37]. For example, melt depletion of sub-continental lithospheric mantle (SCLM) leads to a reduction in Re/Os and subsequent retardation in the growth of ^{187}Os compared to the ambient mantle [30]. On an outcrop- or mineral-scale, the causes of $^{187}Os/^{188}Os$ heterogeneities are less clear. For example, it has been argued that outcrop-scale heterogeneities present in some abyssal peridotites are relatively ancient features reflecting variable melt-depletion of either bulk rocks, or of the phases controlling the budgets of Re, Os (and Pt) (e.g. [16]). In contrast, Standish et al. [33] concluded that variations in $^{187}Os/^{188}Os$ ratios in chromite separates produced from individual samples of abyssal peridotite reflect the combination of generally low initial $^{187}Os/^{188}Os$ for all phases in the rock (~0.12) and variable contamination of the phases with highly radiogenic seawater Os (present day $^{187}Os/^{188}Os \approx 1$).

There is no composition distinction in major or minor elements that can be used to discriminate among the alloy grains with depleted, enriched and average $^{187}Os/^{188}Os$ ratios (Figs. 3 and 4). Consequently, it is unlikely that subsets of the grains were either formed at different times, or by different processes. Although the exact evolution trajectory of $^{187}Os/^{188}Os$ in average upper mantle is still debated, most studies suggest isotopic evolution similar to, or slightly retarded relative to the evolution in chondritic meteorites [15,19,33]. If the Port Orford alloy grains are representative of upper mantle that was last processed during the Phanerozoic, it is clear that this mantle included minor domains that were long-term depleted in Re/Os ratio. For example, the least radiogenic sample of our suite, matrix sample M7, has a $^{187}Os/^{188}Os$ ratio of 0.1174 and a model age calculated relative to the isotopic evolution of carbonaceous chondrites of 1.42 Ga [29]. One of the samples reported by Meibom and Frei [12] has an even older model age of 2.4 Ga.

The data for some alloy grains also indicate domains within the mantle source that were enriched in Re/Os ratio relative to the ambient mantle. Because suprachondritic $^{187}Os/^{188}Os$ ratios of the magnitude observed for the Port Orford suite can be quickly (<5 Ma) generated in a high Re/Os environment, such as mafic crust [38], it is not necessarily true that domains with long-term enriched Re/Os were tapped.

5.3. $^{186}Os/^{188}Os$ ratios

The average $^{186}Os/^{188}Os$ ratio of 0.1198382 for our suite (combined UMd+JSC data, sans depleted sample M7) is elevated 35 ppm relative to our previous best estimate for the chondritic ratio of 0.1198340 [10]. The alloy grains are also slightly enriched in $^{186}Os/^{188}Os$ relative to other upper mantle-derived materials we have previously measured [10,16]. The enrichment is evidently a regional characteristic of the ophiolitic source, given the close correspondence between the average ratio for the grains and the chromitite. The apparent global graininess of $^{186}Os/^{188}Os$ ratios in mantle-derived materials must reflect minor long-term variations in Pt/Os within the convecting upper mantle. Variations in Pt/Os on the order of $\pm10\%$ for 4.5 Ga can account for the variations in $^{186}Os/^{188}Os$ observed. Variations in Pt/Os of this level are observed in chondritic meteorites and recent study of $^{186}Os/^{188}Os$ in chondrites confirms that some chondritic $^{186}Os/^{188}Os$ ratios extend to 0.119839 [39].

The new data provide no evidence for upper mantle domains in the sources of these alloy grains with Pt/Os ratios that were substantially enriched relative to chondritic at some point in the past. No samples are as radiogenic as the more radiogenic Hawaiian and Gorgona lavas. Only sample M7 has a $^{186}Os/^{188}Os$ ratio that cannot be explained as being generated from average Phanerozoic upper mantle. As noted above for its Re/Os ratio, if this grain formed from an upper mantle domain at 162 Ma, that domain must have existed with very low Pt/Os for >1.4 Ga prior to the formation of the grain.

The new ^{186}Os data do not well match the data for Os–Ir–Ru grains reported previously [11,12,14] (Fig. 6). Three options with regard to the discrepancy are tendered: (1) the sample populations examined by the two groups are similar with respect to $^{187}Os/^{188}Os$ but are very different with respect to $^{186}Os/^{188}Os$; (2) our new measurements have a systematic error that tended to lower the average $^{186}Os/^{188}Os$ ratios, and random errors that have biased the ratios to the uniform values observed; or (3) the measurements reported by [12,14] have random and systematic errors that have led to an artificial biasing of sample $^{186}Os/^{188}Os$ ratios to the substantially higher average ratios and greater dispersion compared to our new

data. As discussed above, the similarity in range and average $^{187}Os/^{188}Os$ ratios in the suites of samples analyzed by the two groups suggest similar sample populations. Differences in composition, however, cannot be discounted at this time. To assess the second option, most of our samples were analyzed using two different mass spectrometers. The agreement between results from UMd and JSC are good and suggest that this option is not likely the cause of the discrepancies. As a test for an interlaboratory bias between UMd+JSC versus the University of Copenhagen laboratory used by [12,14], Os from six of the grains examined by this study was sent to R. Frei in Copenhagen for analysis. The UC results for all samples were in good agreement (<50 ppm deviation) with the ratios reported here. We have no mechanism, however, for further testing the third option above. All of the Os extracted from samples with suprachondritic Os measured by [12,14] was reportedly exhausted (R. Frei, personal communication, 2004).

Meibom and Frei [12] and Meibom et al. [14] reported that coupled, positive ^{186}Os–^{187}Os correlations for Os–Ir–Ru alloy grains from NW California and SW Oregon are consistent with mixing between an ancient reservoir that is depleted relative to chondrites in both $^{186}Os/^{188}Os$ and $^{187}Os/^{188}Os$ ratios, and a reservoir that is conversely enriched. If all of the grains originated in the upper mantle, both the depleted and enriched reservoirs must also reside in the upper mantle. These authors used this argument to conclude that other coupled systems, such as the trends reported for Hawaiian picrites and Gorgona komatiites [20,21], also are likely the result of mixing between the same upper mantle reservoirs. If correct, this conclusion would weigh heavily against the interpretation we have favored that the Hawaiian and Gorgona trends are best explained as a consequence of mixing between suprachondritic Os derived from the outer core and Os derived from the ambient upper mantle [20,21]. We note, however, that, if our new data are representative of the Port Orford grains and Os in the upper mantle in general, then there is no evidence that positive ^{186}Os–^{187}Os correlations can be produced via mixing of Os reservoirs within the upper mantle, and indeed, the Pt–Re–Os systematics of the alloy grains would have little bearing on the issue of the origin of coupled trends present in lavas generated from presumed mantle plumes.

5.4. Origin of Port Orford alloy grains

Bird and Bassett [4] speculated that the Port Orford alloy grains may either be primordial or formed during early, or subsequent deep mantle Earth processes. Given the distinctly non-primordial Os isotopic compositions of the grains (e.g. [40]), this option is no longer tenable. The lack of a coupled ^{186}Os–^{187}Os trend for the grains indicates that derivation from the outer core, as suggested by [11], or from mixed sources that includes an ancient global reservoir, as suggested by [12] are also not viable interpretations for these data.

Meibom et al. [13,14] and Brenker et al. [7] presented ^{187}Os isotopic, and mineralogic evidence to contend that alloy grains from southwestern Oregon and California formed within the upper mantle in a supra-subduction zone setting. Our new Os data are permissive of this interpretation. The average ^{187}Os/^{188}Os ratio for our suite of grains matches that of the average ratio previously reported [13] and is consistent with the average composition of Os determined for other materials that may sample the convecting portion of the upper mantle, e.g. ophiolites, abyssal peridotites and orogenic lherzolites [15,19,31]. Not only do the ratio averages match that of the convecting upper mantle, a large majority of grains have ^{187}Os/^{188}Os ratios within $\pm 2\%$ of the mean value of 0.124, suggesting that the provenance of the grains is dominated by Os of a composition that is typical of convecting upper mantle during the Mesozoic [19].

If formed in the convecting upper mantle, the grains with depleted Os isotopic compositions require that this mantle contain at least modest-size domains with long-term, sub-chondritic Re/Os and Pt/Os ratios. That these domains exist is not surprising. Previous studies of abyssal peridotites have reported samples with subchondritic ^{187}Os/^{188}Os ratios and Pt/Os ratios [15,16,33]. Peridotites with strongly depleted ^{187}Os/^{188}Os ratios are also present in orogenic lherzolites [31]. Further, some peridotite xenoliths from the subcontinental lithospheric mantle also have extremely depleted ^{187}Os/^{188}Os ratios [30]. Subchondritic compositions have been reported for chromitites from the mantle sections of both Proterozoic [36] and Phanerozoic [18,19] ophiolites. As noted by Meibom et al. [13], a typical alloy grain contains the quantity of Os that could be concentrated from approximately 1 m^3 of peridotite. That study concluded that homogenization processes within the upper mantle must be incapable of removing Os isotopic heterogeneities on m^3 volumes. Our results are consistent with this interpretation. The limited number of grains with subchondritic compositions, however, indicates that such depleted domains are relatively rare. The 1–2.5 Ga ^{187}Os model ages of the more depleted grains reported here and in Meibom and Frei [12] indicate that such heterogeneities can survive in the convecting mantle for extensive periods of time.

The timing and processes leading to the generation of Os with suprachondritic ^{187}Os/^{188}Os ratios in the suite are more difficult to constrain. Such Os could be generated over long periods of time in small domains with modest enrichments in Re/Os relative to chondritic. Alternately, enriched Os could be created within a short time interval via derivation from mafic rocks with high Re/Os. For example, pyroxenitic veins within the mantle have been suggested to provide ^{187}Os-enriched melt to some mid-ocean ridge basalts and ocean island basalts [23,41]. The low Os content of most mafic rocks, however, means that the more radiogenic compositions would have to have involved concentration of the Os from much greater volumes of mantle rocks. Radiogenic ^{187}Os could even be transported into mantle peridotites via volatile transport from the mafic portions of a subducting slab (e.g. [37,42]).

6. Conclusions

Osmium–Ir–Ru alloy grains collected from placers near Port Orford, Oregon, can be structurally divided into matrix and lamellae [4]. The matrix and the lamellae are chemically disparate, most notably with respect to variations in the concentrations of Fe, and proportions of Os, Ir and Ru contained within grains. Individual grains can contain both matrix and lamellae. Variations in ^{187}Os/^{188}Os ratios were examined within grains using laser ablation ICP-MS. No isotopic heterogeneities within individual matrix or lamellae grains were discovered above the resolution limit of $\pm 0.1\%$. In addition, matrix and lamellae

intergrowths within a single cluster are also isotopically identical.

The uniformity of Os isotopic compositions within individual alloy grains and the cluster suggests that they were constructed from Os, and presumably also Ir and Ru, that may have been concentrated from relatively small domains within the convecting upper mantle as sampled by the Mesozoic-age Josephine ophiolite. The concentration mechanism remains unknown. One possibility is that the grains formed during the serpentinization processes associated either with seafloor processes or the obduction process. Alternately the grains could have crystallized from magma, collecting Os, Ir and Ru from a large-volume magma chamber. The minimum sizes of the domains from which these elements could have been concentrated are on the order of several m^3. The new Os isotopic data and the major element data provide no new constraints with regard to the processes involved, although the presence of the intergrowths noted by Bird and Bassett [4], along with the silicate and oxide inclusions noted by Brenker et al. [7] are probably most consistent with a magmatic origin.

In contrast to previous studies, the $^{186}Os/^{188}Os$ ratios of the grains examined here are uniform within analytical uncertainties. While 35 ppm higher than previous upper mantle estimates, the average $^{186}Os/^{188}Os$ ratio is within the range of chondritic meteorites. These results provide no evidence for a significant reservoir within the upper convecting mantle that has a suprachondritic $^{186}Os/^{188}Os$ ratio.

Acknowledgements

Appendix A. Supplementary data

Supplementary data associated with this article can be found, in the online version, at doi:10.1016/j.epsl.2004.11.009.

References

[1] H.W. Stockman, P.F. Hlava, Platinum-group minerals in alpine chromitites from southwestern Oregon, Econ. Geol. 79 (1984) 491–508.

[2] L.J. Cabri, D.C. Harris, Zoning in Os–Ir alloys and the relation of the geological and tectonic environment of the source rocks to the bulk Pt:Pt+Ir+Os ratio for placers, Can. Mineral. 13 (1975) 266–274.

[3] L.J. Cabri, D.C. Harris, T.W. Weiser, Mineralogy and distribution of platinum-group mineral (PGM) placer deposits of the world, Explor. Min. Geol. 5 (1996) 73–167.

[4] J.M. Bird, W.A. Bassett, Evidence of a deep mantle history in terrestrial osmium–iridium–ruthenium alloys, J. Geophys. Res. 85 (1980) 5461–5470.

[5] D.C. Peck, R.R. Keays, Geology, geochemistry, and origin of platinum-group element chromitite occurrences in the Heazlewood River Complex, Tasmania, Econ. Geol. 85 (1990) 765–793.

[6] D.C. Peck, R.R. Keays, Insights into the behavior of precious metals in primitive, S-undersaturated magmas—evidence from the Heazlewood River Complex, Tasmania, Can. Mineral. 28 (1990) 553–577.

[7] F.E. Brenker, A. Meibom, R. Frei, On the formation of peridotite-derived Os-rich PGE alloys, Am. Mineral. 88 (2003) 1731–1740.

[8] G.H. Riley, S.E. Delong, Osmium isotopes in geology, Int. J. Mass Spectrom. Ion Phys. 4 (1970) 297–304.

[9] C.J. Allègre, J.M. Luck, Osmium isotopes as petrogenetic and geological tracers, Earth Planet. Sci. Lett. 48 (1980) 148–154.

[10] R.J. Walker, J.W. Morgan, E. Beary, M.I. Smoliar, G.K. Czamanske, M.F. Horan, Applications of the $^{190}Pt–^{186}Os$ isotope system to geochemistry and cosmochemistry, Geochim. Cosmochim. Acta 61 (1997) 4799–4808.

[11] J.M. Bird, A. Meibom, R. Frei, T.F. Nägler, Osmium and lead isotopes of rare OsIrRu minerals: derivation from the core-mantle boundary region? Earth Planet. Sci. Lett. 170 (1999) 83–92.

[12] A. Meibom, R. Frei, Evidence for an ancient osmium isotopic reservoir in Earth, Science 296 (2002) 516–518.

[13] A. Meibom, N.H. Sleep, C.P. Chamberlain, R.G. Coleman, R. Frei, M.T. Hren, J.L. Wooden, Re–Os isotopic evidence for long-lived heterogeneity and equilibration processes in the Earth's upper mantle, Nature 419 (2002) 705–708.

[14] A. Meibom, R. Frei, N.H. Sleep, Osmium isotopic compositions of Os-rich platinum group element alloys from the Klamath and Siskiyou Mountains, J. Geophys. Res. 109 (2004).

[15] J.E. Snow, L. Reisberg, Os isotopic systematics of the MORB mantle—results from altered abyssal peridotites, Earth Planet. Sci. Lett. 133 (1995) 411–421.

[16] A.D. Brandon, J.E. Snow, R.J. Walker, J.W. Morgan, T.D. Mock, $^{190}Pt–^{186}Os$ and $^{187}Re–^{187}Os$ systematics of abyssal peridotites, Earth Planet. Sci. Lett. 177 (2000) 319–335.

[17] J.-M. Luck, C.J. Allègre, Osmium isotopes in ophiolites, Earth Planet. Sci. Lett. 107 (1991) 406–415.

[18] J.E. Snow, G. Schmidt, E. Rampone, Os isotopes and highly siderophile elements (HSE) in the Ligurian ophiolites, Italy, Earth Planet. Sci. Lett. 175 (2000) 119–132.

[19] R.J. Walker, H.M. Prichard, A. Ishiwatari, M. Pimentel, The osmium isotopic composition of convecting upper mantle deduced from ophiolite chromitites, Geochim. Cosmochim. Acta 66 (2002) 329–345.

[20] A.D. Brandon, M.D. Norman, R.J. Walker, J.W. Morgan, [186]Os–[187]Os systematics of Hawaiian picrites, Earth Planet. Sci. Lett. 172 (1999) 25–42.

[21] A.D. Brandon, R.J. Walker, I.S. Puchtel, H. Becker, M. Humayun, S. Revillon, [186]Os–[187]Os systematics of Gorgona Island komatiites: implications for early growth of the inner core, Earth Planet. Sci. Lett. 206 (2003) 411–426.

[22] G. Ravizza, J. Blusztajn, H.M. Prichard, Re–Os systematics and platinum-group element distribution in metalliferous sediments from the Troodos ophiolite, Earth Planet. Sci. Lett. 188 (2001) 369–381.

[23] A.D. Smith, Critical evaluation of Re–Os and Pt–Os isotopic evidence on the origin of intraplate volcanism, J. Geodyn. 36 (2003) 469–484.

[24] J.M. Bird, M.S. Weathers, Josephinite-specimens from Earth's core? Earth Planet. Sci. Lett. 28 (1975) 51–64.

[25] C.E. Feather, Mineralogy of platinum-group minerals in Witwatersrand, South-Africa, Econ. Geol. 71 (1976) 1399–1428.

[26] J.M. Brenan, D. Andrews, High-temperature stability of laurite and Ru–Os–Ir alloy and their role in PGE fractionation in mafic magmas, Can. Mineral. 39 (2001) 341–360.

[27] D.C. Harris, L. Cabri, The nomenclature of the natural alloys of osmiridium, iridium, and rutherium based on new compositional data of alloys from world-wide occurrences, Can. Mineral. 12 (1973) 104–112.

[28] G.D. Harper, J.S. Saleeby, M. Heizler, Formation and emplacement of the Josephine ophiolite and the Nevadan orogeny in the Klamath Mountains, California–Oregon: U/Pb zircon and [40]Ar/[39]Ar geochronology, J. Geophys. Res. 99 (1994) 4293–4321.

[29] S.B. Shirey, R.J. Walker, The Re–Os isotope system in cosmochemistry and high-temperature geochemistry, Annu. Rev. Earth Planet. Sci. 26 (1998) 423–500.

[30] R.J. Walker, R.W. Carlson, S.B. Shirey, F.R. Boyd, Os, Sr, Nd, and Pb isotope systematics of southern African peridotite xenoliths: implications for the chemical evolution of subcontinental mantle, Geochim. Cosmochim. Acta 53 (1999) 1583–1595.

[31] L.C. Reisberg, J.P. Lorand, Longevity of subcontinental mantle lithosphere from osmium isotope systematics in orogenic peridotite massifs, Nature 376 (1995) 159–162.

[32] K. Hattori, S.R. Hart, Osmium-isotope ratios of platinum-group minerals associated with ultramafic intrusions—Os isotopic evolution of the oceanic mantle, Earth Planet. Sci. Lett. 107 (1991) 499–514.

[33] J.J. Standish, S.R. Hart, J. Blusztajn, H.J.B. Dick, K.L. Lee, Abyssal peridotite osmium isotopic compositions from Cr-spinel, Geochem. Geophys. Geosyst. 3 (2002) (doi:10.1029/2001GC000161; 24 p.).

[34] C.E. Martin, Osmium isotopic characteristics of mantle-derived rocks, Geochim. Cosmochim. Acta 55 (1991) 1421–1434.

[35] R.J. Walker, E.J. Hanski, J. Vuollo, J. Liipo, The Os isotopic composition of Proterozoic upper mantle:evidence for chondritic upper mantle from the Outokumpu ophiolite, Finland, Earth Planet. Sci. Lett. 141 (1996) 161–173.

[36] A. Tsuru, R.J. Walker, A. Kontinen, P. Peltonen, E. Hanski, Re–Os isotopic systematics of the 1.95 Ga Jormua Ophiolite Complex, northeastern Finland, Chem. Geol. 164 (2000) 123–141.

[37] A.D. Brandon, R.A. Creaser, S.B. Shirey, R.W. Carlson, Osmium recycling in subduction zones, Science 272 (1996) 861–864.

[38] A. Gannoun, K.W. Burton, L.E. Thomas, I.J. Parkinson, P. van Calsteren, P. Schiano, Osmium isotope heterogeneity in the constituent phases of mid-ocean ridge basalts, Science 303 (2004) 70–72.

[39] A.D. Brandon, The osmium isotopic composition of Tagish Lake and other chondrites, implications for late terrestrial planetary accretion, Lunar and Planetary Science Conference XXXIV, 2003, abstract #1776.

[40] M.I. Smoliar, R.J. Walker, J.W. Morgan, Re–Os ages of group IIA, IIIA, IVA, and IVB iron meteorites, Science 271 (1996) 1099–1102.

[41] P. Schiano, J.-L. Birck, C.J. Allègre, Osmium–strontium–neodymium–lead isotopic covariations in mid-ocean ridge basalt glasses and the heterogeneity of the upper mantle, Earth Planet. Sci. Lett. 150 (1997) 363–379.

[42] A.D. Brandon, H. Becker, R.W. Carlson, S.B. Shirey, Isotopic constraints on time scales and mechanisms of slab material transport in the mantle wedge: evidence from the Simcoe mantle xenoliths, Washington, USA, Chem. Geol. 160 (1999) 387–408.

[43] T.B. Massalski, Binary alloy phase diagrams, in: H. Okamoto, P.R. Subramanian, L. Lacpzak (Eds.), Hf–Re to Zn–Zr, 2nd ed., ASM International, Materials Park, OH, 1990, 2224 pp.